their preferred solution gives a slope of $b = 11.54$. They argue that the choice of the slope has negligible effect on the distance modulus, but as shown in Table 2 their steeper slope makes a difference of $\Delta(m-M) = +0.13$. The sensitivity of the solution to the slope has also been emphasized by Richter and Huchtmeier[6]. (Aaronson and Mould[1] have not included in the quoted error their estimated zero point error of 0.2 mag; with this additional error included our error estimates do not deviate significantly.)

In an investigation of the slope of the blue Tully–Fisher relation, Richter and Huchtmeier[6] have found a slope of $b = 7.17$ and from a large sample of 66 Virgo galaxies a Virgo cluster modulus of $(m-M)_{\text{Virgo}} = 31.82 \pm 0.14$. Adopting their slope, using the local calibrators as shown in Table 1, and including only the 48 Virgo galaxies of type Sab to Sd of their sample, we find $(m-M)_{\text{Virgo}} = 31.66 \pm 0.26$ (the error here includes the error of the constant term $a = -19.82 \pm 0.23$).

It is reassuring for the 21 cm linewidth method, that it yields Virgo cluster distances for IR and blue magnitudes that are almost the same. The mean value of $(m-M)_{\text{Virgo}} = 31.57 \pm 0.25$ agrees well with our independently determined value $(m-M)_{\text{Virgo}} = 31.67 \pm 0.26$ (ref. 7), but we emphasize that the 21 cm method should be viewed with caution until it is better understood why the Hubble-type dependence has not yet been found in the radio data, but is clearly present in the optical results[10].

If one carries the distance scale beyond the Virgo cluster out to the Coma cluster by means of relative distance indicators given in Table 4, one obtains a value of the Hubble constant which must essentially be free of all irregularities of the expansion field and thus must be very close to the global value of H_0. Adopting a Virgo modulus based on the IR Tully–Fisher relation leads then to $H_0 = 58 \pm 10$, or $H_0 = 55 \pm 9$ on the basis of the IR and blue Virgo modulus. Both solutions lie well within the error range of the preferred value of $H_0 = 50 \pm 7$ (ref. 7).

There are remaining problems with the Tully–Fisher relation. In addition to the problem of the dependence on galactic type previously mentioned, there is (1) the possibility that the relation is not the same for field and cluster galaxies[24,25], and (2) the problem that the true intrinsic dispersion of the relation, if large, discriminates against intrinsically faint galaxies of a given linewidth and leads to an underestimate of the distances. It is therefore a matter of personal judgement how much weight one wants to attribute to the method. It is in any case, however, satisfactory to see that the 21 cm linewidth method, as it begins to mature, leads to results which are now consistent with the established distance scale.

This agreement is particularly satisfactory because it reinforces the time-scale agreement between the Hubble time of H_0^{-1} (50) $= 19.5 \times 10^3$ Myr the age of the chemical elements at $\sim 20 \times 10^3$ Myr (ref. 26), and the age of the globular clusters in our Galaxy at $\sim 18 \times 10^3$ Myr (refs 27, 28).

G.A.T. is a visiting associate of Mount Wilson and Las Campanas Observatories, Carnegie Institution, and acknowledges support from the Swiss NSI.

Received 24 June; accepted 8 November 1983.

1. Aaronson, M. & Mould, J. *Astrophys. J.* **265,** 1–17 (1983).
2. Dressler, A. Preprint, Mount Wilson and Las Campanas Observatories (1983).
3. Sandage, A. *Astr. J.* **88,** 1108–1125 (1983).
4. Sandage, A. & Carlson, G. *Astrophys. J. Lett.* **267,** L25–28 (1983).
5. Sandage, A. *Astr. J.* (in the press).
6. Richter, O.-G. & Huchtmeier, W. K. *Astr. Astrophys.* (in the press).
7. Sandage, A. & Tammann, G. A. *Astrophysical Cosmology* (eds Brück, H. A., Coyne, G. V. & Longair, M. S.) 23–81 (Pontifica Academia Scientiarum, 1982); *Astrophys. J.* **256,** 339–345 (1982).
8. Tammann, G. A. & Sandage, A. *Highlights Astr.* **6,** 301–313 (1983).
9. Sandage, A. & Tammann, G. A. *A Revised Shapley-Ames Catalog of Bright Galaxies*, 6 (Carnegie Institution, Washington, 1981).
10. Rubin, V. C. *IAU Symp.* No. 100, 3–8 (1983).
11. Sandage, A. & Tammann, G. A. *Astrophys. J.* **151,** 531–545 (1968).
12. Sandage, A. & Tammann, G. A. *Astrophys. J.* **157,** 683–708 (1969).
13. Madore, B. F. Talk at IAU General Assembly, Patras (1982).
14. McAlary, C. W. & Madore, B. F. Preprint, Steward Observatory, Tucson (1983).
15. Graham, J. A. *Astrophys. J.* **252,** 474–480 (1982).
16. Graham, J. A. *Highlights Astr.* **6,** 209–216 (1983).
17. Aaronson, M., *et al. Astrophys J. Suppl.* **50,** 241–262 (1982).
18. Mould, J., Aaronson, M. & Huchra, J. *Astrophys. J.* **238,** 458–470 (1980).
19. Aaronson, M., Mould, J. & Huchra, J. *Astrophys. J.* **237,** 655–665 (1980).
20. Yahil, A., Sandage, A. & Tammann, G. A. *Physical Cosmology* (eds Balian, R., Audouze, J. & Schramm, D. N.) 158 (North Holland, Amsterdam, 1980).
21. Aaronson, M., Persson, S. E. & Frogel, J. A. *Astrophys. J.* **245,** 18–24 (1981).
22. Tifft, W. G. & Gregory, S. A. *Astrophys. J.* **205,** 696–708 (1976).
23. Yahil, A., Sandage, A. & Tammann, G. A. *Astrophys. J.* **217,** 903–915 (1977).
24. Kraan-Korteweg, R. C. *Astr. Astrophys.* **125,** 109–111.
25. Giovannelli, R. C. *IAU Symp.* No. 104, 273–278 (1983).
26. Thielemann, F.-K., Metzinger, J. & Klapdor, H. V. *Z. Phys.* **A309,** 301–317 (1983).
27. Sandage, A. *Astrophys. J.* **252,** 553–573 (1982).
28. VandenBerg, D. A. *Astrophys. J. Suppl.* **51,** 29–65 (1983).
29. Tammann, G. A. & Sandage, A. *Astrophys. J.* **151,** 825–860 (1968).
30. Sandage, A. & Tammann, G. A. *Astrophys. J.* **194,** 223–243 (1974).
31. Sandage, A. *Astr. J.* **88,** 1569–1578 (1983).
32. Sandage, A. & Hardy, E. *Astrophys. J.* **183,** 743–757 (1973).
33. Weedman, D. W. *Astrophys.* **203,** 6–13 (1976).
34. Visvanathan, N. & Sandage, A. *Astrophys. J.* **216,** 214–226 (1977).
35. Tammann, G. A. *Supernovae: A Survey of Current Research* (eds Rees, M. J. & Stoneham, R. J.) 371–403 (1982).

A helix stop signal in the isolated S-peptide of ribonuclease A

Peter S. Kim & Robert L. Baldwin

Department of Biochemistry, Stanford University Medical Center, Stanford, California 94305, USA

The isolated S-peptide (residues 1–20 of ribonuclease A) is known to show partial α-helix formation in aqueous solutions at low temperatures. We show here that the helix is limited to certain residues, including ones that are helical in the intact protein, and that a functional helix termination signal exists in the isolated peptide.

THE α-helix is the most abundant unit of secondary structure in proteins. Most α-helices are quite short: the average length of α-helices in proteins is about 11 residues[1]. In contrast, the average length of α-helices is much longer in synthetic polypeptides (about 100 residues at the transition midpoint)[2], and therefore, α-helix termination signals exist in proteins. The nature of these helix termination signals is of fundamental interest with respect both to the mechanism of protein folding and the prediction of folding from amino acid sequence. An important question concerning the mechanism of protein folding is whether the helix start and stop signals function at early stages in folding when the α-helices and β-sheets are first formed, or whether tertiary interactions are required to fix the ends of helices.

The X-ray structures of RNase A[3] and of RNase S[4] show that RNase contains three short helices. [RNase S is an enzymatically active derivative of RNase A cleaved at the peptide bond between residues 20 and 21; the proteolysis products can be separated and are referred to as the S-peptide (residues 1–20) and the S-protein (residues 21–124)[5].] The structure of interest here is the α-helix formed by residues 3–13 (counting residues containing at least one α-helical H-bond). The crystal structure shows that the amide proton of Asp 14 (the next H-bond donor at the C-terminal end of the 3–13 helix) is H-bonded to the

0028–0836/84/040329—06$01.00

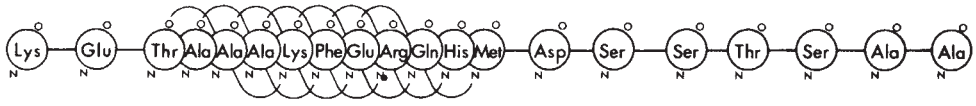

Fig. 1 Amino acid sequence of S-peptide (1–20), showing the α-helix formed by these residues in native RNase A[3] and RNase S[4]. S-peptide (1–20) was prepared and purified for us by V. MacCosham. RNase A (Sigma Type 1-AS, lot no. 81F-8015) was purified[18] and then digested with Subtilisin Carlberg (Sigma Type VIII, lot no. 48C-0164)[19]. S-peptide was purified by ion exchange chromatography (SP-Sephadex C25 in 0.01 M HCl; 0.05–1.0 M NaCl gradient) and by gel filtration (Sephadex G-25 fine in 0.01 M HCl). Two peptides were separated using the purification procedure above, and amino acid analysis (performed at the Department of Biochemistry and Biophysics, University of California, Davis) indicated that the peptides were S-peptide (1–19) and S-peptide (1–20) (see ref. 20). All experiments reported here were made using purified S-peptide (1–20).

carbonyl oxygen of Val 47 in a tertiary interaction (contrast Fig. 4 f of ref. 6). Thus, this tertiary interaction holds residue 14 in a non-helical conformation. One would like to know whether this tertiary interaction is required for the localization of the 3–13 helix, or if a functional helix termination signal exists in the absence of tertiary interactions (for example in an early protein folding intermediate).

One direct approach for investigating the nature of helix termination signals is to study the folding of protein fragments. Until recently, however, this has not been possible because even large fragments of single-domain proteins have been found to be unfolded in aqueous solutions[7,8]. Moreover, 'host-guest' data for α-helix formation in water by synthetic polypeptides[9] indicate that short α-helices (<20 residues) are always unstable in water, regardless of the amino acid composition. These data have led to the conclusion that secondary structure in protein fragments is not stable in the absence of stabilizing tertiary structure interactions.

Nevertheless, both the C-peptide of RNase A (residues 1–13, obtained by cyanogen bromide cleavage at Met-13, yielding HSer-13 lactone as the C-terminal residue), and the S-peptide (residues 1–20) show partial helix formation in aqueous solutions as judged by circular dichroism (CD) spectra and by ^{1}H nuclear magnetic resonance (NMR) studies[10–13]. Some characteristics of the helix formed by the C-peptide are as follows. (1) Up to ~30% helix content is observed in water near 0 °C[11], which is 1,000 times greater than the helix content predicted using data from host–guest studies. (2) Helix formation is strongly dependent on temperature, and C-peptide is essentially unfolded in aqueous solutions at 25 °C[10,11]. (3) Equilibrium sedimentation measurements show that C-peptide is monomeric at concentrations up to 2 mg ml^{-1} in conditions in which helix formation occurs (1 °C, 0.1 M ionic strength)[10]. (4) The *p*H dependence of helix stability follows a bell-shaped curve[11], with maximum helix formation occurring near *p*H 5. A possible explanation for this *p*H dependence has been given[11]: a salt bridge between the ionized sidechains of Glu 9$^-$ and His 12$^+$ could stabilize the helix.

Here we use S-peptide (1–20), which contains the first 20 amino acids of RNase A, to ask whether the α-helix formed by the isolated peptide stops near residue 13 (the last residue of this helix in native RNase A or RNase S). Five residues with low helical propensity occur in a stretch next to the 3–13 helix (residues 14–18, see Fig. 1). Although studies of helix formation in random copolymers allow some amino acid residues to be classified as 'helix formers' and others as 'helix breakers', the reported stability constant (s) values for helix growth span a very narrow range ($s = 0.5$–1.3 for all residues studied)[9]. The 'cooperative length' of an α-helix is about 100 residues[2] $= 1/\sigma^{1/2}$, where σ is the helix nucleation constant; $\sigma \sim 10^{-4}$ for all residues studied[9]. Predicted distributions of helix length for short peptides (including end effects) containing a single residue type are discussed by Schellman[14]. For a 20 residue peptide, these results show that a significant fraction of the α-helices formed will include all 20 residues, in the absence of helix termination signals.

To determine whether the α-helix formed by S-peptide (1–20) is localized, we have followed the ^{1}H-NMR chemical shifts of various sidechain groups as the helix is unfolded. The helices formed by S-peptide (1–20) and C-peptide lactone can be unfolded by increasing temperature[11,13], GuHCl[12], or urea, as we report here. Since the stability of the S-peptide (1–20) helix is *p*H dependent[13], we have also monitored the ^{1}H-NMR chemical shifts of sidechain groups as the helix content is changed by varying *p*H. Of particular interest are those amino acid residue types that are present both within and outside the native 3–13 α-helix (Fig. 1). These include the alanine residues (Ala 4, 5, and 6 are in the helix of native RNase A, whereas Ala 19 and 20 are not), and the threonine residues (Thr 3 is in the native helix and Thr 17 is not). The β-CH_3 group of alanine is physically close to the α-helix backbone, and the alanine β-CH_3 resonance is expected to shift with helix formation, as has already been observed for Ala 4, 5, and 6 in the C-peptide lactone helix[12]. The γ-CH_3 resonance of Thr 3 also shifts as the C-peptide lactone helix is formed[11], and here we ask whether the Thr 17 (γ-CH_3) resonance shows a comparable helix shift.

Table 1 Comparison between NMR helix shifts and CD changes in S-peptide (1–20) and C-peptide lactone (1–13).

NMR resonance	Peptide	Helix shift $\Delta\delta$ (p.p.m.)*	Molar peptide CD change $\Delta[\theta]_{222}$ (deg cm^2 dmol^{-1})†	Normalized helix shift $\Delta\delta/\Delta[\theta]_{222}$	Ratio (R) of normalized helix shift S-Peptide (1–20): C-Peptide lactone‡
Thr 3 (γCH_3)	S-peptide (1–20)	0.071	4.30×10^4	1.65×10^{-6}	1.07
Thr 3 (γCH_3)	C-peptide (lactone)	0.103	6.69×10^4	1.54×10^{-6}	
Phe 8 (ϕH)§	S-peptide (1–20)	−0.051	4.30×10^4	-1.19×10^{-6}	1.04
Phe 8 (ϕH)	C-peptide (lactone)	−0.076	6.69×10^4	-1.14×10^{-6}	

* Difference in chemical shift between 4 °C and 47 °C, at the optimum *p*H for helix formation. S-peptide (1–20) data are for *p*H 3.8. Data for C-peptide lactone (*p*H 5.0) are from ref. 11. Temperature dependence of chemical shift, in absence of helix formation, not taken into account.

† Difference in $[\theta]_{222}$ per mole peptide between 3 °C and 40 °C (*p*H 3.8) for S-peptide (1–20)[13] and between 3 °C and 45 °C (*p*H 5.0) for C-peptide lactone[11].

‡ Predicted value for R is 1.0 if the helix is localized to the same residues in both peptides and if the helix shifts are the same for both peptides at 100% helix formation. If the helices propagate to the ends of both peptides, then R is predicted to be ≤ 0.63 ($\frac{12}{19}$, corresponding to the ratio of the number of peptide carbonyl groups). Due to end effects on the apparent molar ellipticity of an α-helix (see ref. 24 and refs therein), R will be <0.63 if the helices include all residues of both peptides.

§ There are six visible resonance lines for Phe 8, and only three of them shift significantly with helix formation[11]. Values are reported for the middle resonance of these three.

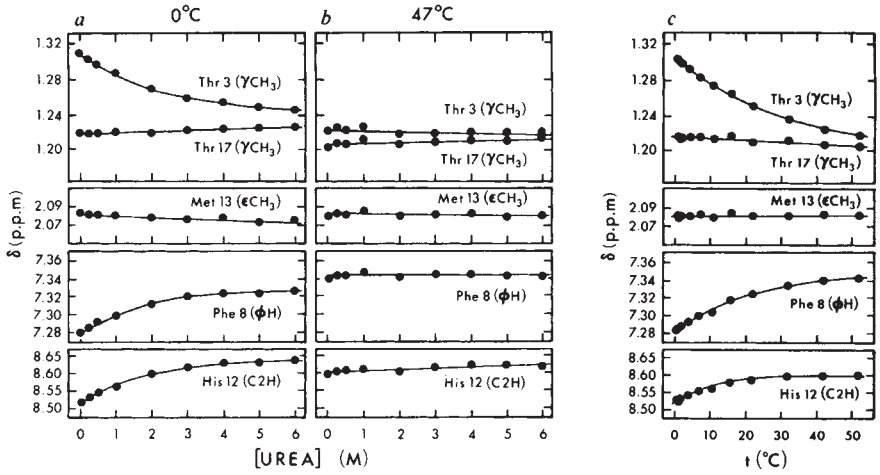

Fig. 2 *a*, Urea dependence of ^{1}H-NMR chemical shift for some side-chain resonances in S-peptide (1–20): 0 °C, *p*H 3.8, 0.1 M NaCl, D_2O. *b*, Urea dependence: 47 °C, *p*H 3.8, 0.1 M NaCl, D_2O. *c*, Temperature dependence of ^{1}H-NMR chemical shift for some side-chain resonances in S-peptide (1–20): *p*H 3.8, 0.1 M NaCl, D_2O. The average chemical shift for the threonine γ-CH_3 doublets are shown. There are six visible resonance lines for Phe 8 (ϕH), and only three of them shift significantly with helix formation. The middle resonance of these three is shown.

Methods: All samples contained 0.1 M NaCl in D_2O. *p*H was adjusted with DCl or NaOD, and *p*H values refer to meter readings without isotope corrections. Urea and GuHCl were Schwarz-Mann ultrapure grade. Urea-d_4 and GuDCl-d_6 were prepared by repeated lyophilization from D_2O (Liquid Carbonic, 99.7% C). All other chemicals were reagent grade. Fourier-transform proton NMR spectra were recorded on a modified Bruker 360 MHz instrument at the Stanford Magnetic Resonance Facility. All chemical shifts are reported relative to the internal standard, TSP. Corrections were made for the *p*H dependence of the TSP signal[21]. Resolution-enhanced NMR spectra were obtained by multiplication of the free-induction decay with either a double exponential[22] or a sine bell function[23]. Damping of the free-induction decay in the presence of urea was observed (contrast ref. 20), but did not affect the spectra of the peptide. Resonance assignments have been or will be given elsewhere[20] (A. Bierzynski *et al.* manuscript in preparation). The Thr 17 (γ-CH_3) resonance was assigned by comparing the spectra of S-peptide (1–15) and S-peptide (1–20) in the unfolded state (5.0 M GuDCl, 0° or 47 °C).

Side-chain resonances

The optimum conditions for α-helix formation in aqueous solutions of S-peptide (1–20), as judged by CD, are *p*H 3.8, 0 °C[13]. As urea is added in these conditions, some side-chain resonances show chemical shift changes while others do not (Fig. 2*a*). The side-chain resonances of Thr 3, Phe 8 and His 12 show changes in chemical shift as the helix is unfolded with urea. However, when the α-helix is already thermally unfolded at 47 °C, urea does not affect the chemical shifts of these resonances (Fig. 2*b*).

In contrast to Thr 3, the side-chain resonance of Thr 17 does not change as the helix is unfolded (Fig. 2). Thus, Thr 17 is probably not in the α-helix formed by the isolated S-peptide (1–20). End effects (helix fraying) are not sufficient to explain the difference observed between Thr 3 and Thr 17, because Thr 3 is the third residue from the amino-terminus and Thr 17 is the fourth residue from the carboxyl-terminus.

The S-CH_3 resonance of Met 13 does not shift as urea is added (Fig. 2). However, the lack of a helix shift for Met 13 is difficult to interpret for two related reasons. (1) The S-CH_3 sidechain group of methionine is four bonds removed from the peptide backbone, and it may be possible for the helix to form without perturbing the magnetic environment of the S-CH_3 protons. (2) We do not have a positive control demonstrating a helix shift for a methionine S-CH_3 resonance, whereas with other resonances (for example threonine γ-CH_3), a positive control exists. It is therefore not possible to tell whether Met 13 is contained in the helix formed by isolated S-peptide (1–20). In native RNase A, Met 13 is the last residue in the α-helix. His 12 (ring C2H resonance) does show a helix shift (Fig. 2). The β-CH_3 resonances of Ala 4, 5, 6, 19, and 20 are not well separated in spectra taken in urea at high temperatures, or at high urea concentrations, 0 °C, and are therefore not depicted in Fig. 2.

The α-helices formed by both C-peptide lactone and S-peptide (1–20) unfold with increasing temperature[11,13]. Figure 2*c* depicts the temperature dependences of the chemical shifts for the resonances shown previously, at *p*H 3.8. The residues that show a helix shift for urea-induced unfolding (Fig. 2*a*) also show a temperature-induced helix shift (Fig. 2*c*). In particular, the Thr 17 resonance, which does not show a urea-induced helix shift (Fig. 2*a*), also does not show a temperature-induced shift (Fig. 2*c*), supporting the suggestion that the S-peptide (1–20) helix is localized.

Guanidine deuterochloride (GuDCl) is known to affect the chemical shifts of many side-chain resonances, and these changes are often not attributable to the unfolding of structure. Moreover, the effects of GuDCl on chemical shifts are dependent on neighbouring groups, suggesting that the effects are related to the binding of GuDCl to the peptide[12]. Our GuDCl titrations of S-peptide (1–20) at 37 °C, where the helix is thermally unfolded, also show GuDCl-induced changes in chemical shift (Fig. 3*b* and 4*b*) and some of these resonances continue to change between 3–5 M GuDCl, where S-peptide (1–20) should be in a 'random coil' conformation.

In addition, GuDCl appears to cause a 'salt effect' on the chemical shifts between 0 and 1 M GuDCl that does not appear to be related to helix structure for the following reasons. (1) The effect is observed even at 37 °C, where the helix is thermally unfolded (Fig. 3*b* and Fig. 4*b*). (2) Essentially all resonances show the salt-effect. These GuDCl-induced chemical shifts may be caused in part by effects of GuDCl on the internal standard (TSP). Both GuDCl and TSP are charged, and we have observed NaCl-dependent shifts of the TSP resonance relative to acetone or dioxane.

When the GuDCl titrations are performed at 0 °C (favouring helix formation), some resonances show changes in chemical shift that evidently are caused by helix unfolding (Fig. 3*a* and Fig. 4*a*). To determine the changes in chemical shift caused by helix unfolding, we have subtracted the GuDCl dependence of the chemical shifts at 37 °C, in the absence of helix formation, from the dependence at 0 °C where the helix is populated. The temperature difference curves for the GuDCl titrations are depicted in Fig. 3*c*. As was found with urea and temperature, the side-chain resonances of Thr 3, Phe 8, and His 12 show helix shifts with GuDCl, whereas those of Met 13 and Thr 17 do not (Fig. 3*c*).

An advantage of using GuDCl is that resonances are spread out which arise in similar regions of the NMR spectrum. In particular, the five alanine β-CH_3 groups (Ala 4, 5, 6, 19, and 20) give rise to ten resonance lines in the NMR spectrum of S-peptide (1–20). There is considerable overlap of these resonances in the spectrum, under conditions in which the helix is unfolded by urea or temperature. The interaction of GuDCl with the peptide results in the separation of these resonances in the spectrum (Fig. 4). The resonances listed as Ala I, II, III correspond to Ala 4, 5, 6 respectively (see Fig. 4 legend).

In S-peptide (1–20), as in C-peptide lactone[12], Ala 4, 5, and 6 show significant helix shifts; the difference between the GuDCl titration curves at 0° and at 37 °C is shown for each resonance in Fig. 4*c*. In marked contrast, Ala 19 and 20 do not show measurable helix shifts (Fig. 4*c*), supporting further the sugges-

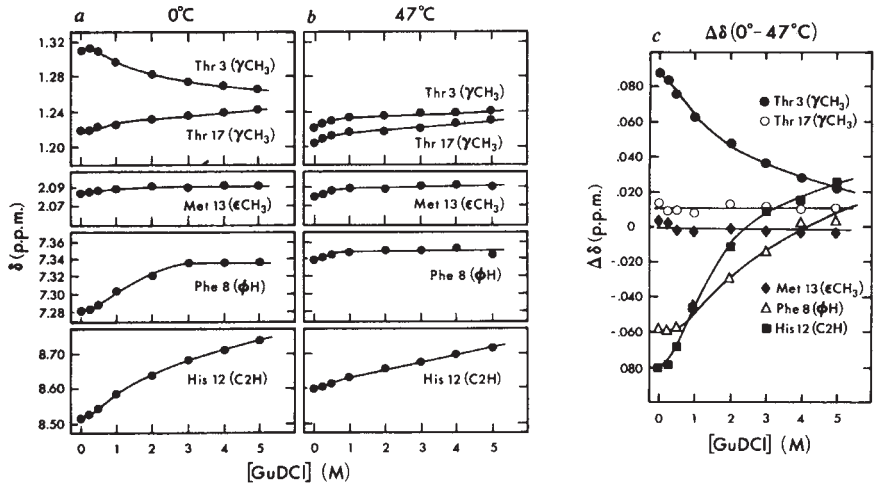

Fig. 3 GuDCl titrations of S-peptide (1–20). *a*, 0 °C, *p*H 3.8, 0.1 M NaCl, D_2O. *b*, 47 °C, *p*H 3.8, 0.1 M NaCl, D_2O. *c*, Δδ (0–47 °C); the difference in chemical shift between 0 °C and 47 °C.

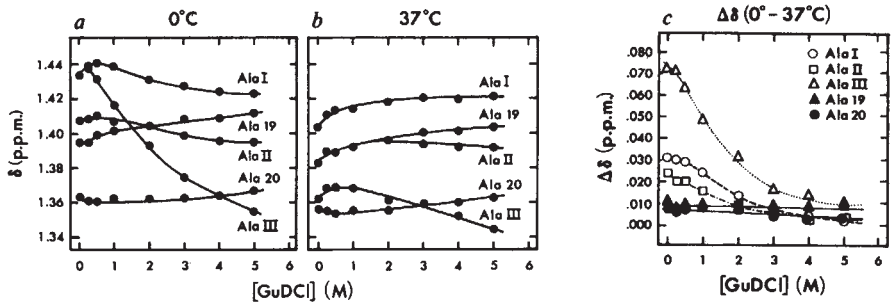

Fig. 4 GuDCl titrations of the alanine β-CH_3 resonances in S-peptide (1–20). *a*, 0 °C, *p*H 3.8, 0.1 M NaCl, D_2O. *b*, 37 °C, *p*H 3.8, 0.1 M NaCl, D_2O. *c*, Δδ (0–37 °C); the difference in chemical shift between 0 °C and 37 °C. The average chemical shift for each alanine β-CH_3 doublet is shown. The resonances numbered Ala I, II, III correspond to Ala 4, 5 and 6 respectively. These assignments were made, after submission of this paper, using a synthesized peptide containing deuterated alanine. The resonance assignments of Ala 19 and 20 were made by comparing the spectra of S-peptide (1–15) and S-peptide (1–20) in the unfolded state (5.0 M GuDCl, 0° or 37 °C) to locate Ala 19 and 20, and by *p*H titration of the α-COOH group of Ala 20, to locate Ala 20.

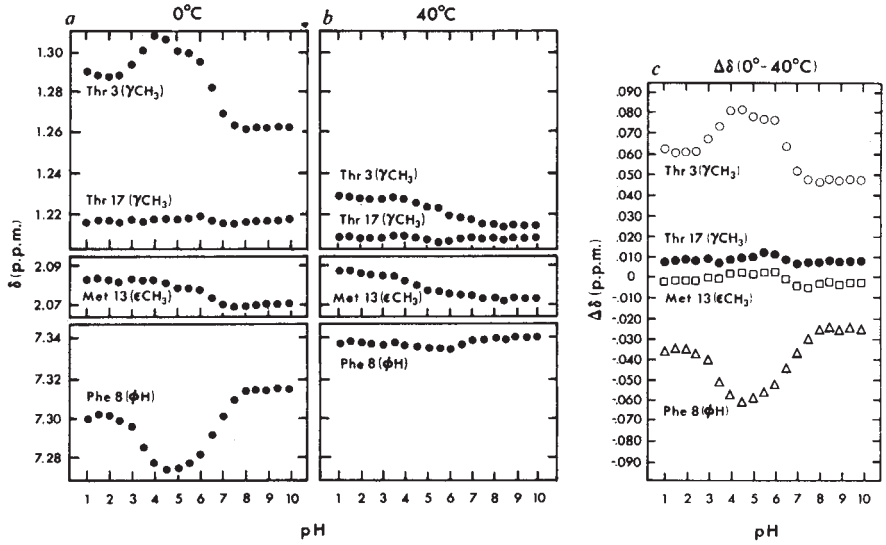

Fig. 5 *p*H titration of S-peptide (1–20). *a*, 0 °C, 0.1 M NaCl, D_2O. *b*, 40 °C, 0.1 M NaCl, D_2O. *c*, Δδ (0–40 °C); the difference in chemical shift between 0 °C and 40 °C. The *p*H titration of His 12 (C2H) is dominated by changes in chemical shift due to the titration of the imidizole ring and is not depicted. The Ala β-CH_3 resonances are not well separated in some conditions and are not shown.

tion that the α-helix formed by isolated S-peptide (1–20) is localized. The alanine β-CH_3 resonances are particularly useful indicators of helix formation. Only one bond separates the alanine β-CH_3 group from the peptide backbone. Moreover, rotation about this bond ($C_\alpha - C_\beta$) is fast on the NMR time scale under all conditions investigated here. A small linear shift is observed for Ala 20 as GuDCl is added, but this shift is clearly distinct from the helix shifts observed for Ala 4, 5, and 6 (Fig. 4*c*). The linear GuDCl shift for Ala 20 is probably related to the fact that Ala 20 is the last residue in the peptide, and contains the α-COO^- group.

Comparison with CD results

A direct comparison between the molar ellipticity change (222 nm) caused by helix formation for C-peptide lactone and for S-peptide (1–20) is not yet possible, for the following reasons. (1) Only partial helix formation has been observed for either peptide, even in the optimal helix-forming conditions. For C-peptide lactone, a helix content of 30% at *p*H 5.0, 0 °C, has been estimated from CD measurements. It is likely that, in these conditions, 30% of the molecules are helical and 70% are in a random coil conformation; almost all resonances of C-peptide lactone show shifts as the helix is formed[11] (A.

Bierzynski *et al.*, manuscript in preparation). Any comparison between the CD changes on helix formation for the two peptides depends critically on the relative stabilities of the helices formed by the two peptides. (2) The *p*H–stability profiles for C-peptide lactone[11] and for S-peptide[13] differ in important respects: the optimal *p*H is 5.0 for C-peptide lactone but 3.8 for S-peptide. Consequently, a comparison between helix stabilities at any given *p*H is arbitrary. A comparison between the molar ellipticity changes on helix formation by the two peptides has been made earlier, at *p*H 5.5, by Brown and Klee[15], who were not aware either of the strong *p*H dependence of helix stability or of the different *p*H–stability profiles of the two helices. Also, they studied helix formation in an unresolved mixture of C-peptide lactone and C-peptide carboxylate, without knowing the striking difference between the helix-forming properties of these two peptides (contrast ref. 13).

We have made an approximate comparison between the molar ellipticity changes on helix formation for C-peptide lactone and S-peptide (1–20) in the following way. We assume that the residues within the helix have the same structure in the helical conformation of both peptides and consequently that the helix shifts for 100% helix formation are the same for both helices, measured for any of several side-chain resonances. From the observed helix shifts, we calculate a ratio for the extent of helix formation for the two peptides. This ratio is then compared to the ratio of ellipticity changes (per mole peptide). The results (Table 1) show that these two ratios are the same, indicating that approximately the same number of residues participate in helix formation in both peptides. This is consistent with the conclusion that the helix in S-peptide (1–20) terminates before Thr 17 and possibly near Met 13.

*p*H dependence of helix stability

As mentioned above, the stabilities of both the S-peptide (1–20) helix and the C-peptide lactone helix are strongly dependent on *p*H. However, the *p*H dependence of $[\theta]_{222}$ is more complex in S-peptide (1–20)[13] than in C-peptide lactone[11]. At low temperatures, where the helix is populated, the *p*H dependence of $[\theta]_{222}$ shows a complex curve[13], in contrast with the almost symmetric bell-shaped curve found with C-peptide lactone[11]. When either peptide is thermally unfolded (40–45 °C), $[\theta]_{222}$ is essentially independent of *p*H[11,13]. These results suggest that charged residue(s) which affect helix stability exist in S-peptide (1–20) that are not present in C-peptide lactone.

We have monitored the *p*H dependence of chemical shift for some resonances of S-peptide (1–20) at 0 °C and 40 °C, and the results are depicted in Fig. 5. At 40 °C, some resonances show *p*H-dependent chemical shifts (Fig. 5*b*) that are unrelated to helix formation. We again take the difference in chemical shift between 0 °C and 40 °C, to obtain the shifts that are due to helix formation. The results (Fig. 5*c*) show that both Thr 3 and Phe 8 give *p*H-dependent helix shifts that are qualitatively similar to the *p*H dependence of $[\theta]_{222}$ for S-peptide (1–20)[13]. In contrast, Thur 17 and Met 13 (S-CH_3) do not show a significant *p*H-dependent shift in the temperature difference plot (Fig. 5*c*). These data agree with the conclusion that S-peptide (1–20) contains a functional helix termination signal, and they suggest that the same residues are contained within the helix at all *p*H values where helix formation is observed.

NMR and helix termination

In the present study, we have monitored side-chain resonances and have measured 'helix shifts' (changes in chemical shift caused by alterations in the helix stability with temperature, urea, GuDCl, or *p*H) to determine whether a given residue participates in helix formation. The fact that self-consistent results are obtained with all four methods of changing the helix content lends support to this procedure. Nevertheless, the results with the S-CH_3 resonance of Met 13 point out a possible danger in using this approach: the group may be too far removed from the peptide backbone to show a significant change in chemical shift on helix formation. In this regard, the results with the β-CH_3 resonances of Ala 4, 5, 6, 19, and 20 are particularly valuable in indicating helix termination within the peptide, because the β-CH_3 group of Ala is very close to the peptide backbone of the helix. In order to study these five Ala resonances, it was necessary to make use of the ability of GuDCl to spread out the chemical shifts of groups of the same residue type.

Helix termination signal

Measurements of the equilibrium constant for nucleation (σ) in homopolymers and random copolymers[9] indicate that σ is always very small ($\sigma \sim 10^{-4}$). The cooperative length of an α-helix in aqueous solutions is thus predicted to be about 100 residues[2] ($=1/\sigma^{1/2}$). In contrast, our results indicate that the helix formed by S-peptide (1–20) is localized to certain residues. The features of the naturally occurring amino acid sequence of S-peptide (1–20) that are responsible for helix termination are of obvious interest.

In order to understand the mechanism of helix termination in S-peptide (1–20), we will need to have a more detailed description of termination. One wants to know at which residue the helix terminates and whether termination is gradual (spread out over a few residues) or abrupt. In future work it will be useful to use ^{13}C-enriched amino acids to monitor backbone resonances, and to monitor additional side-chain resonances with two-dimensional NMR techniques. One would also like to find conditions (perhaps with new derivatives of the S-peptide and C-peptide) in which helix formation goes to completion for those residues in the helix. Then the molar CD changes for helix formation in different peptides can be compared directly, and the NMR results can be extended by measuring amide proton exchange rates and nuclear Overhauser effects.

We consider here two contrasting models for helix termination in peptides that may also play a role in protein folding. Our present data are largely consistent with a simple helix termination mechanism in which the amino acid sequence increases the helix nucleation constant (σ), and therefore decreases the cooperative length of the helix (for example, increasing σ to 10^{-2} would decrease the cooperative length to 10 residues). Then, a stretch of residues with low helix propensity (for example, residues 14–18 of S-peptide) would prevent propagation of the helix. The observed stabilities of the C-peptide lactone and S-peptide (1–20) helices are 1,000-fold greater than that predicted using the value of $\sigma \sim 10^{-4}$ obtained from polymer studies. If σ were larger in S-peptide, for example due to specific interactions between sidechains, then the increased stability and termination of the S-peptide (1–20) helix could be explained. On the other hand, the mechanism of helix termination may directly involve specific interactions between sidechain groups. For example, model building shows that a H-bonding interaction between the sidechains of His 12^+ and Asp 14^- would prevent propagation of the S-peptide (1–20) helix past residue 13. The *p*H dependence of S-peptide (1–20) is more complex than that of C-peptide lactone[13], and the additional ionizing groups in S-peptide (1–20) involve only Asp 14 and the α-COO^- group of Ala 20. More work is needed to distinguish between these and other possible explanations of helix termination in S-peptide.

Mechanism of protein folding

Studies of C-peptide lactone[11] and S-peptide[13] have demonstrated that isolated units of secondary structure can have significant stability in water. The data presented here suggest that functional termination signals can exist in isolated units of secondary structure. These results are consistent with the simple framework model for protein folding in which the amino acid sequence directly determines the positions of the α-helices and β-sheets, and these secondary structures then pair to form the tertiary fold. Since C-peptide lactone and S-peptide provide the first examples of α-helix formation and termination in aqueous solutions of a short peptide fragment of a protein, it is important to point out that they provide only isolated examples, and many

more examples will be needed to base conclusions about the folding mechanism.

These data are encouraging with regard to predicting secondary structure from amino acid sequence because they suggest that helix formation in the isolated S-peptide is localized to the same, or nearly the same, residues as in native RNase A. It is interesting that present schemes for predicting secondary structure are more successful in finding the locations of helices than in defining their endpoints[17]. Experiments of the type described here, with peptides of specified amino acid sequence, may provide clues about the nature of helix termination signals.

We thank Drs K. Kuwajima and D. E. Wemmer for discussions, S. G. Boxer for use of his computing facilities and V. MacCosham for technical assistance. This work was supported by NIH grant 2 RO1 GM 19988-22. P.S.K. is a predoctoral fellow of the Medical Scientist Training Program. Use of the Stanford Magnetic Resonance Facility (supported by NSF grant GP 23633 and NIH grant RR 00711) is acknowledged.

Note added in proof: A recent ^{1}H-NMR study[25] (published after submission of this article) of helix formation by S-peptide (1–19) agrees with our conclusion that the helix is limited to certain residues including the helical residues of RNase A.

Received 5 September; accepted 10 October 1983.

1. Schulz, G. E. & Schirmer, R. H. *Principles of Protein Structure* (Springer, New York, 1979).
2. Poland, D. & Scheraga, H. A. *Theory of Helix-Coil Transitions in Biopolymers* (Academic, New York, 1970).
3. Wlodawer, A., Bott, R. & Sjölin, L. *J. biol. Chem.* **257**, 1325–1332 (1982).
4. Richards, F. M. & Wyckoff, H. W. *Atlas of Molecular Structures in Biology 1. Ribonuclease-S* (Clarendon, Oxford, 1973).
5. Richards, F. M. & Vithayathil, P. J. *J. biol. Chem.* **234**, 1459–1465 (1959).
6. Wyckoff, H. W. *et al. J. biol. Chem.* **245**, 305–328 (1970).
7. Epand, R. M. & Scheraga, H. A. *Biochemistry* **7**, 2864–2872 (1968).
8. Taniuchi, H. & Anfinsen, C. B. *J. biol. Chem.* **244**, 3864–3875 (1969).
9. Scheraga, H. A. *Pure appl. Chem.* **50**, 315–324 (1978).
10. Brown, J. E. & Klee, W. A. Biochemistry **10**, 470–476 (1971).
11. Bierzynski, A., Kim, P. S. & Baldwin, R. L. *Proc. natn. Acad. Sci. U.S.A.* **79**, 2470–2474 (1982).
12. Bierzynski, A. & Baldwin, R. L. *J. molec. Biol.* **162**, 173–186 (1982).
13. Kim, P. S., Bierzynski, A. & Baldwin, R. L. *J. molec. Biol.* **162**, 187–199 (1982).
14. Schellman, J. A. *J. chem. Phys.* **62**, 1485–1494 (1958).
15. Brown, J. E. & Klee, W. A. *Biochemistry* **8**, 2876–2879 (1969).
16. Blackburn, P. & Moore, S. *The Enzymes* Vol. 15, 317–433 (Academic, New York, 1983).
17. Schulz, G. E. *et al. Nature* **250**, 140–142 (1974).
18. Garel, J.-R. *Eur. J. Biochem.* **70**, 179–189 (1976).
19. Doscher, M. S. *Meth. Enzym.* **11**, 640–648 (1967).
20. Kuwajima, K. & Baldwin, R. L. *J. molec. Biol.* **169**, 281–297 (1983).
21. DeMarco, A. *J. Mag. Res.* **26**, 527–528 (1977).
22. Ferrige, A. G. & Lindon, J. C. *J. Mag. Res.* **31**, 337–340 (1978).
23. DeMarco, A. & Wüthrich, K. *J. Mag. Res.* **24**, 201–204 (1976).
24. Chen, Y.-H., Yang, J. T. & Chau, K. H. *Biochemistry* **13**, 3350–3359 (1974).
25. Rico, M. *et al. FEBS Lett.* **162**, 314–319 (1983).

Activation of a translocated human c-*myc* gene by an enhancer in the immunoglobulin heavy-chain locus

Adrian C. Hayday*, Stephen D. Gillies*, Haruo Saito*, Charles Wood*, Klas Wiman†, William S. Hayward† & Susumu Tonegawa*

* Center for Cancer Research and Department of Biology, Massachusetts Institute of Technology, Cambridge, Massachusetts 02139, USA
† Memorial Sloan-Kettering Cancer Center, New York, New York 10021, USA

A tissue-specific transcriptional enhancer element that is associated with the human immunoglobulin heavy-chain locus is defined. In a non-Hodgkin's lymphoma that contains a translocated c-myc *gene this enhancer is retained on the 14q$^+$ chromosome and occurs within sequences shown to activate previously cryptic promoters of the* c-myc *gene.*

A FUNCTIONAL immunoglobulin gene is generated somatically during the differentiation of B lymphocytes by a set of developmentally regulated gene rearrangements[1]. The major function of these rearrangements is to generate a diverse set of complete immunoglobulin genes from a limited number of inherited gene segments.

Another important role of these rearrangements has recently been identified at least for the mouse immunoglobulin heavy-chain genes[2–4]. In an individual B lymphocyte and its progenies, only one of a few hundred copies of the variable (V) gene segments is expressed. This activation of a specific V gene segment results from its direct rearrangement into the vicinity of a transcriptional enhancer element that is located upstream of the constant (C) region gene segments, between the joining (J) segments and the switch (S) region. Interestingly, the immunoglobulin gene-associated enhancer functions in a tissue-specific manner, suggesting a more general involvement of cellular enhancer elements in tissue-specific expression of eukaryotic genes during cell differentiation.

Another biological process in which gene rearrangements and enhancer elements may play a critical, albeit adventitious, role is tumorigenesis. A model supporting this notion comes from the studies on the chicken leukaemogenesis induced by the non-acute avian leukosis virus (ALV). By integrating close to the cellular oncogene, c-*myc*, the ALV provirus via its transcriptional promoter or enhancer element can lead to increased levels of c-*myc* transcription[5,6]. It has recently been shown that the c-*myc* gene is translocated into an immunoglobulin locus in certain lymphoid neoplasms of both mice and men[7–12]. Thus, murine c-*myc* gene is recombined into the immunoglobulin heavy-chain locus in BALB/c plasmacytomas characterized by t(12:15) translocations[7,9–11]. Likewise, in a majority of the many Burkitt's lymphomas or non-Hodgkin's lymphomas characterized by t(8:14) (q24; q32) translocations, the c-*myc* gene is recombined into the immunoglobulin heavy-chain locus[8,11,12]. It has generally been considered that in these and other neoplasms where nonrandom chromosomal translocations have been observed, c-*onc* genes are activated by the translocations[13–15].

To understand the relationship between the translocation and activation of a c-*myc* gene we have been analysing the structure and expression of normal and translocated human c-*myc* genes. The results presented here demonstrate that the human immunoglobulin heavy-chain locus carries a transcriptional enhancer element analogous to its mouse counterpart, and that this enhancer element may be playing a direct part in the activation of the translocated c-*myc* gene in some lymphoid neoplasms.

c-*myc* translocation in Manca cells

The non-Hodgkin's lymphoma, Manca[16], shows a chromosome translocation (t(8:14)(q24; q32)) that is characteristic of many

0028–0836/84/040334—07$01.00